EPJ Web of Conferences **151**, 06001 (2017) DOI: 10.1051/epjconf/201715106001
LAM-16

Asymmetrical bonding in liquid Bi disentangled by inelastic X-ray scattering

Masanori Inui[1,*], *Yukio* Kajihara[1], *Shuji* Munejiri[1], *Shinya* Hosokawa[2], *Ayano* Chiba[3], *Koji* Ohara[4], *Satoshi* Tsutsui[4], and *Alfred Q. R.* Baron[5,4]

[1]Graduate School of integrated Arts and Sciences, Hiroshima University, Higashi-Hiroshima, Hiroshima 739-8521, Japan
[2]Department of Physics, Graduate School of Science and Technology, Kumamoto University, Kumamoto 860-8555, Japan
[3]Department of Physics, Keio University, Yokohama 223-8522, Japan
[4]Japan Synchrotron Radiation Research Institute, SPring-8, Sayo-gun, Hyogo 679-5198, Japan
[5]Materials Dynamics Laboratory, RIKEN SPring-8 Center, Sayo-gun, Hyogo 679-5148, Japan

Abstract. The structure of liquid Bi has been debated in relationship with the Peierls distortion, as crystalline Bi takes A7 structure. A recent *ab initio* molecular dynamics simulation for liquid Bi predicted a flat-topped profile of the acoustic dispersion curve. To confirm the prediction, we have carried out inelastic x-ray scattering (IXS) for liquid Bi. The dynamic structure factor obtained by the IXS exhibits a distinct inelastic excitation of the longitudinal acoustic mode up to 14 nm^{-1} and the dispersion curve of the excitation energy obtained by the memory function analysis becomes a flat-topped one. We found that a linear chain model including the interatomic interaction with the second nearest neighbors can explain the flat-topped profile. The result suggests that the anomalous dispersion curve in liquid Bi arises from local anisotropy related to the Peierls distortion in the crystalline phase. .

1 Introduction

Bi belongs to the same group as As in the periodic table of elements, and the local structure of liquid Bi has been discussed from a view-point of the Peierls distortion [1]. The Peierls distortion is realized in a A7 crystalline structure type comprising three short and three long bonds in a distorted simple cubic lattice to gain the electronic energy.

The structure factor $S(Q)$ of liquid Bi, where Q is momentum transfer, exhibits a shoulder at high momentum transfer side of the first maximum (see Fig. 3) [2–4], in contrast to a symmetrical profile of simple liquid metals. The origin of the shoulder in $S(Q)$ of liquid Bi was theoretically studied and it was found that an effective pair potential with a ridge in the repulsive component could reproduce the shoulder [5, 6]. Later, an *ab initio* molecular dynamics (AIMD) simulation for liquid Bi [7] revealed that longer and shorter bonds produce a distinct shoulder at the first peak in $S(Q)$.

Atomic dynamics in liquid Bi had been studied by inelastic neutron scattering (INS) experiments. Most recently, Sani *et al.* [8] carried out INS experiments at $Q \leq 6$ nm^{-1} and

*e-mail: masinui@hiroshima-u.ac.jp

reported the dynamic structure factor $S(Q,E)$, where E is energy transfer, with good statistics. The $S(Q,E)$ exhibits the inelastic excitations of the acoustic mode dispersing with Q. However, this result did not fix conflicting INS results obtained in 1980's: Dahlborg and Olsson [9, 10] reported no distinct inelastic excitation of the acoustic mode in $S(Q,E)$ at $Q > 6$ nm^{-1}, while Shibata *et al.* [11] reported experimental observation of the acoustic excitations up to 12 nm^{-1}. Later Dzugutov and Dahlborg [5] reported that there appears no distinct acoustic excitation at $Q > 6$ nm^{-1} with a classical molecular dynamics simulation (CMD), consistent with the INS results by Dahlborg and Olsson.

Contrary to the CMD result, Souto *et al.* [7] reported that inelastic excitations of the acoustic mode survive up to 14 nm^{-1} in $S(Q,E)$ obtained by an *ab initio* molecular dynamics (AIMD) simulation. Furthermore the AIMD simulation for liquid Bi predicted an intriguing dispersion curve of the acoustic mode with a flat-topped profile, which is much different from a sinusoidal profile in simple liquid metals [12]. To investigate the behavior of the acoustic excitation in liquid Bi, we carried out inelastic x-ray scattering (IXS) experiments. A high-resolution IXS technique allows us to avoid the kinematic constraints of INS and to obtain good spectra out to large energy transfer. The technique is also advantageous for measurements at extreme conditions such as high temperatures and high pressures owing to a small beam size of approximately 0.1 mm in diameter. Details of the IXS results have already been reported in Ref.[13]. In this article, we report the results of the acoustic mode in liquid Bi briefly and present results obtained by $S(Q,E)$ near the first peak position of $S(Q)$ that are not published.

2 Experimental procedure

The IXS experiments were conducted at the high-resolution IXS beamline (BL35XU) at SPring-8 in Japan [14]. Backscattering at the Si (11 11 11) reflection provided a beam of approximately 10^{10} photons/sec in a 0.8 meV bandwidth onto the sample. The energy of the incident beam and the Bragg angle of the backscattering were 21.747 keV and approximately 89.98°, respectively. The spectrometer resolution was approximately 1.5 meV depending on the analyzer crystal, and it was experimentally determined by scattering from polymethyl methacrylate (PMMA). Q resolution, ΔQ, was set to be 0.45 and 1.0 nm^{-1} (full width) for $Q \leq 11$ and $Q > 11$ nm^{-1}, respectively.

X-ray diffraction measurements using monochromatized high-energy x-ray were carried out at BL04B2/SPring-8 [15], to obtain $S(Q)$. Details of the data processing are described in Ref. [13].

Liquid Bi of 99.999% purity was mounted in a single-crystalline sapphire cell of Tamura-type [16] that was carefully machined to provide a 0.04 mm sample thickness. The cell was placed in "Marburg" chamber [17]. IXS spectra were measured at 573 and 1023 K [18] in pure He atmosphere at 0.1 MPa. The background spectra were measured at 573 K with an empty cell. After the absorption correction, the backgrounds were subtracted from the data, and $S(Q,E)/S(Q)$ were obtained. More details were described in Ref. [13].

3 Computer simulations

AIMD simulations were performed at 573 K using Quantum ESPRESSO package [19], which is based on the density functional theory, plane waves and pseudopotentials. The generalized gradient approximation(GGA) [20] was adopted for the exchange-correlation energy. We used the norm-conserving pseudopotential Bi.pbe-hgh.UPF [21] for the electron-ion interaction with five valence electrons, $6s^2 6p^3$. The plane-wave cutoff energy for the electronic

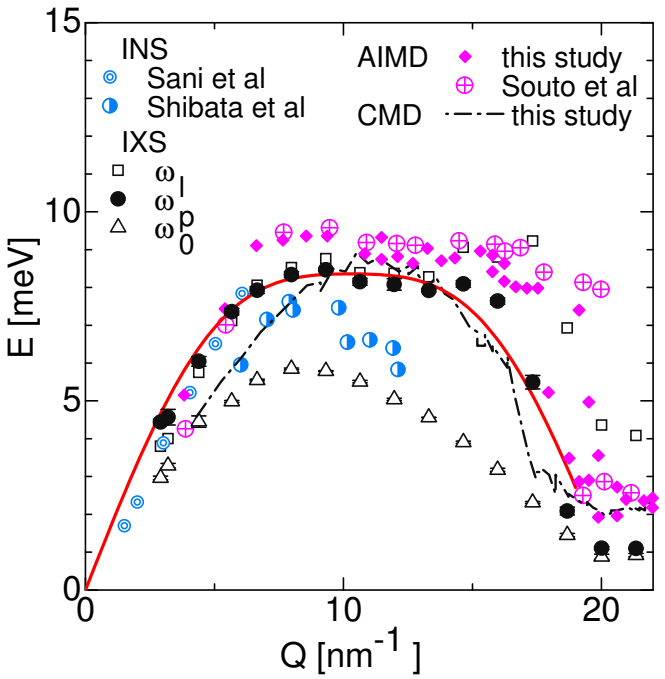

Figure 1. $\omega_\ell(Q)$ (open squares), $\omega_\mathrm{p}(Q)$ (black circles) and $\omega_0(Q)$ (open triangles) obtained by IXS results at 573 K. $\omega_\mathrm{p}(Q)$ by AIMD simulations of this study and that at 600 K [7] is indicated by diamonds and circles with cross, respectively. Also shown are the excitation energy obtained by INS by Sani *et al.* (double circles) and by Shibata *et al.* (circles with half moon), and CMD (dash-dotted line). A bold red curve denotes the dispersion relation obtained by a regular chain model with two force constants.

wavefunctions was 15 Ry. The Γ point was only used to sample the Brillouin zone of the MD supercell. We used 128 Bi atoms in a cubic MD cell with periodic boundary conditions. The length of the side of the MD cell was 1.6422 nm. The MD simulation was performed on the ground-state Born-Oppenheimer surface at 573 K for 32 000 steps with a time step of 4.8 fs, and reproduced $S(Q,E)$ at $Q \geq 3.8$ nm^{-1} with quality as good as that by Souto *et al* [7]. We also carried out a CMD simulation at 573 K using the model potential reported in [5] for a system with 256 particles. To obtain $S(Q,E)$, the simulation was performed for 60 000 steps with a time step of 2.4 fs. More details are described in Ref. [13].

4 Results and discussion

4.1 The acoustic dispersion

The integration of $S(Q,E)$ obtained by IXS was carefully compared with $S(Q)$ obtained independently by our own x-ray scattering experiment. By adjusting the integration at 8 nm^{-1} with $S(Q)$, we obtained $S(Q,E)$ of the absolute scale. Then $S(Q,E)$ obtained by IXS was compared with that by INS. Our data nicely agree with those by Sani *el al.* [8]. The difference is that INS spectra are truncated at an energy where inelastic excitations still exist, probably owing to the kinematic constraint of INS. Our results exhibit that the inelastic excitation is

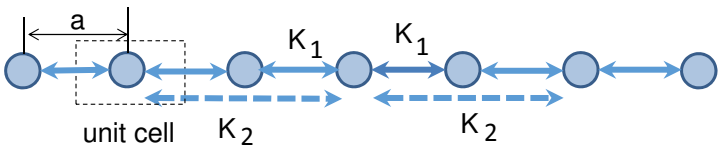

Figure 2. A schematic illustration of a linear chain connected with springs between the first and second nearest neighbors.

visible at $Q \geq 6$ nm^{-1} and it disperses with increasing Q. Hence the prediction by Souto *et al.* [7] was experimentally confirmed. Details are shown in Ref. [13].

To determine the excitation energy of the acoustic mode, $S(Q,E)/S(Q)$ experimentally obtained should be deconvoluted with the resolution function. We tried three model functions; (a) the memory function formalism with two viscous decay channels [22–25], (b) a model function consisting of single Lorentzian and single damped harmonic oscillator (DHO) [26], and (c) a model function consisting of single Lorentzian and two DHO's. Hereafter, we present the results using (a). Details of these model functions are described in Ref. [13]. Using the memory function formalism, the excitation energy of the acoustic mode, $\omega_{\rm p}(Q)$, was defined as the peak position of the current-current correlation function deduced from the deconvoluted $S(Q,E)/S(Q)$.

Figure 1 shows $\omega_{\rm p}(Q)$ of liquid Bi at 573 K as a function of Q, with the normalized second frequency moment, $\omega_0(Q)$, and the normalized fourth frequency moment $\omega_\ell(Q)$. $\omega_0(Q)$ and $\omega_\ell(Q)$ are fitting parameters in the memory function analysis. The figure also depicts the excitation energies obtained by the AIMD and CMD simulations, and those of INS measurements by Sibata *et al.* [11] and Sani *et al.* [8]. As shown in the figure, $\omega_{\rm p}(Q)$ obtained by IXS linearly disperses up to 7 nm^{-1} This dispersion curve is consistent with that obtained by INS by Sani *et al*. $\omega_{\rm p}(Q)$ deviates from the linear dispersion and stays at approximately 8.5 meV at $10 \leq Q \leq 15$ nm^{-1}. A flat region in the dispersion curve is consistent with the prediction by the AIMD simulations by Souto *et al.* [7] although the AIMD results lie at energies slightly higher than black circles. The IXS results surely confirm the theoretical prediction of a flat-topped dispersion curve.

As shown in Fig.1, the peak positions of the current-current correlation function obtained by CMD (a dash-dotted curve) agree with $\omega_{\rm p}(Q)$ (black circles) at approximately 10 nm^{-1}. With decreasing Q, however, real excitation energies of the acoustic modes deviate much from the CMD results at approximately 5 nm^{-1}. This result suggests that the effective pair potential, able to reproduce characteristics in S (Q), cannot exactly simulate the atomic dynamics in liquid Bi at low Q.

We could related the flat-topped dispersion curve of the acoustic mode in liquid Bi, using a linear chain model. We describe it using the illustration in Fig. 2. A simple linear chain connected by a spring with force constant K_1 gives a sinusoidal dispersion curve expressed by $M\omega^2 = 2K_1(1-\cos Qa)$, where M, ω and a are atomic mass, an excitation energy and a lattice constant, respectively. When the second springs of a force constant K_2 are fixed between the central atom and the second nearest neighbors as shown in the figure, the equation of the dispersion curve is modified as $M\omega^2 = 2K_1(1-\cos Qa)+2K_2(1-\cos 2Qa)$. This equation can reproduce a flat-topped dispersion curve by adjusting parameters K_1, K_2 and a [13]. Although the model is based on a regular structure, the concept of a pseudo-Brillouin zone [27] may support applicability of our model to a disordered structure. A linear chain connected by

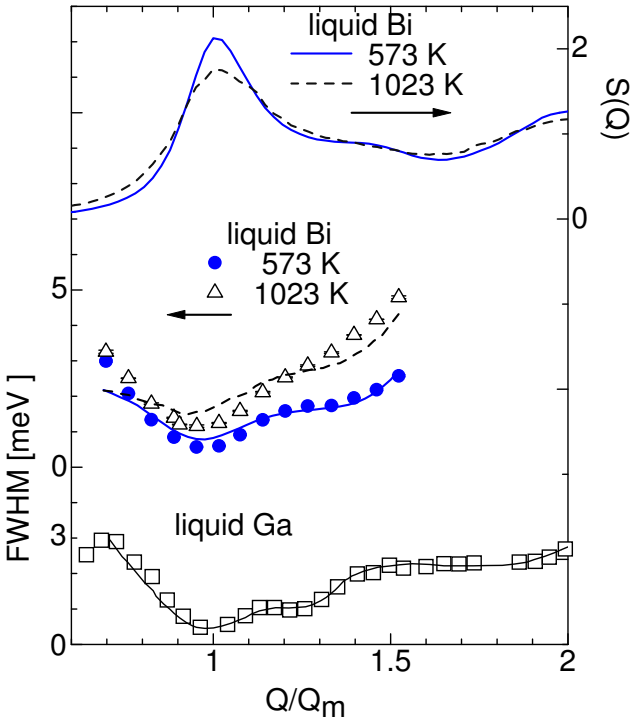

Figure 3. $S(Q)$ (upper curves) and the FWHM of the dynamics structure factor (middle curves and symbols) of liquid Bi at 573 and 1023 K in this work, and the FWHM of liquid Ga (a bottom curve and symbols) reported in [28]. The FWHM denoted by symbols is the IXS results and that denoted by lines is the theoretical optimization by Eq. (1).

strong and weak springs hints the one-dimensional Peierls distortion. Hence, we could relate the flat-topped dispersion curve with the Peierls distortion in liquid Bi.

4.2 Hard-sphere-like dynamics

$S(Q)$ of liquid Bi exhibits the first maximum with a shoulder at higher Q. $S(Q)$ of liquid Ga exhibits a similar profile. Scopigno *et al.* [28] carried out IXS measurements of liquid Ga near the melting point, and analyzed the linewidth of $S(Q, E)$ in high Q region including the $S(Q)$ maximum using an Enskog's theory. The equation given by de Schepper and co-workers [29] expresses the linewidth $z_h(Q)$ as,

$$z_h(Q) = \frac{1}{S(Q)} \frac{D_E Q^2}{1 - j_0(Q\sigma) + 2j_2(Q\sigma)}, \quad (1)$$

where D_E, $j_0(x)$ and $j_2(x)$ are Enskog's diffusion coefficient, zero-th and second order spherical Bessel functions, respectively. D_E is related to Boltzmann diffusion coefficient D_0 as $D_E = D_0/g(\sigma)$, where $g(\sigma)$ is the pair distribution function at a hard sphere diameter σ. By using free parameters of D_E and σ, and $S(Q)$ experimentally obtained, Scopigno *et al.* could reproduce Q dependence of the linewidth well as shown at the bottom of Fig.3. To evaluate

Table 1. The optimized Enskog's diffusion coefficient D_E and hard sphere diameter σ with a packing fraction φ and a number density ρ.

T [K]	D_E [m^2/s]	$\hbar D_E$ [meV nm^2]	σ [nm]	φ	ρ [nm^{-3}]
573	3.6×10^{-9}	2.4×10^{-3}	0.36	0.71	28.9
1023	6.1×10^{-9}	4.0×10^{-3}	0.35	0.63	27.2

the effective mass, D_E expressed by the packing fraction φ [28, 30]

$$D_E = \frac{1}{16}\sqrt{\frac{\pi k_B T}{m}}\left(\frac{6}{\pi\rho\varphi^2}\right)^{\frac{1}{3}}\frac{(1-\varphi)^3}{(1-\varphi/2)}, \quad (2)$$

was used. Here m and ρ are the effective mass and number density, respectively. In a hard sphere model, φ, ρ and σ are related as $\varphi = \pi\rho\sigma^3/6$. In the case of liquid Ga, σ slightly larger than the atomic diameter of Ga, and an effective mass sightly larger than the atomic mass were obtained. These results obtained for liquid Ga were discussed as an indication of existence of dimeric clusters in Ref. [28].

To apply the Enskog's theory, we deconvoluted $S(Q,E)/S(Q)$ with a Lorentzian and the resolution function. Figure 3 shows a full width at half maximum (FWHM) obtained for liquid Bi at 573 (blue circles) and 1023 (open triangles) K as a function of Q/Q_m, where Q_m denotes the first peak position of $S(Q)$. Q_m values of liquid Bi and liquid Ga are 0.21 and 0.25 nm^{-1}, respectively. In our analysis, $S(Q)$ of liquid Bi was our own data obtained by x-ray diffraction measurements shown at the top of the figure. Bold and broken curves at the middle position of the figure denote the optimized fits using eq.(1), where D_E and σ are free parameters as the previous study [28]. As shown in the figure, the best fits reproduce FWHM at 573 K fairly well but does not at 1023 K. Although FWHM denoted by symbols seems to follow the profile of $S(Q)$, the fitting profiles are clearly worse than the results of liquid Ga. The optimized D_E and σ are tabulated in Table 1. σ of liquid Bi is larger than a cutoff distance in $g(r)$, which is approximately 0.29 nm. Asymmetrical bonding consisting of longer and shorter bonds may be inferred in liquid Bi from the optimized σ. However it was not a reasonable result that the effective mass obtained using eq. (2) was much smaller than the atomic mass.

5 Conclusion and future perspective

The present results suggest that a flat-topped dispersion curve observed in liquid Bi can be explained by taking the interatomic force between the second nearest neighbors into account. This result strongly hints asymmetrical bonding in liquid Bi. Symmetry breaking of bonding related to electronic energy levels in a molecule is well known as the Jahn-Teller effect. Hence, local structure may also be distorted in a liquid if a distortion makes the electronic energy lowered, as the case of liquid Bi.

Peierls distortion in liquid Bi has been expected by detailed analysis of the average structure [1]. Such a picture was strongly supported by atomic configurations obtained by AIMD simulations AIMD [7], and primitive analysis for the flat-topped dispersion curve confirmed by the present IXS results. It is very important to study the profiles of acoustic dispersion curves in liquid metals and semiconductors where asymmetrical bonding is expected, in order to understand the present results deeply.

Acknowledgements

The authors would like to thank the Ministry of Education, Culture, Sports, Science and Technology, Japan, for a Grant-in-Aid for Scientific Research. The synchrotron radiation experiments were performed at the SPring-8 with the approval of the Japan Synchrotron Radiation Research Institute (JASRI) (Proposals No. 2011B1314, No. 2010B1173, and No. 2009B1283). M. I. would like to thank The Japan Science Society for Sasakawa Grants for Science Fellows (SGSF).

References

[1] M. Mayo *et al.*, J.Phys:Condens. Matter **25**, 505102 (2013).
[2] M. North *et al.*, J. Phys. C **1**, 1075-1087 (1968).
[3] Y. Waseda and K. Suzuki, Phys. Stat. Sol. B **49**, 339-347 (1972).
[4] Y. Greenberg *et al.*, Euro. Phys. Lett. **86**, 36004 (2009).
[5] M. Dzugutov M and U. Dahlborg, Phys. Rev. A **40**, 4103-4106 (1989).
[6] W. Jank W and J. Hafner, Phys. Rev. B **45**, 2739-2749 (1992).
[7] J. Souto *et al.*, Phys. Rev. B **81**, 134201 (2010).
[8] L. Sani *et al.*, J. Non-Cryst. Solids **353**, 3139-3144 (2007).
[9] U. Dahlborg and L. G. Olsson, Phys. Rev. A **25**, 2712-2720 (1982).
[10] U. Dahlborg and L. G. Olsson, J. Phys. F **13**, 555-561 (1983).
[11] K. Shibata *et al.*, J. Phys. Soc. Jpn. **53**, 899-902 (1984).
[12] T. Scopigno *et al.*, Rev. Mod. Phys. **77**, 881-933 (2005).
[13] M. Inui *et al.*, Phys. Rev. B **92**, 054206 (2015).
[14] A. Q. R. Baron *et al.*, J. Phys. Chem. Solids **61**, 461-465 (2000).
[15] S. Kohara *et al.*, J. Phys.: Condens. Matter **19**, 506101 (2007).
[16] K. Tamura *et al.*, Rev. Sci. Instrum. **70**, 144-152 (1999).
[17] S. Hosokawa and W.-C. Pilgrim, Rev. Sci. Instrum. **72**, 1721-1728(2001).
[18] $S(Q,E)$ at 1023 K was consistent with that obtained by AIMD simulations using 512 atoms by M. Ropo *et al.* [J. Chem. Phys. **145**184502, (2016).]
[19] P. Giannozzi *et al.*, J. Phys.:Condens. Matter **21**, 395502 (2009).
[20] J. P. Perdew *et al.*, Phys. Rev. Lett. **77**, 3865-3868 (1996).
[21] *http://www.quantum-espresso.org.*
[22] D. Levesque *et al.*, Phys. Rev. A **7**, 1690-1700 (1973)
[23] U. Balucani and M. Zoppi *Dynamics of liquid State* (Clarendon press. Oxford) (1994)
[24] T. Scopigno *et al.*, J. Phys.: Condens. Matter **12**, 8009-8034(2000).
[25] F. Bencivenga *et al.*, Phys. Rev. E **75**, 051202 (2007).
[26] B. Fåk B and B. Dorner, Physica B **234-236**, 1107 (1997).
[27] T. Scopigno *et al.*, Phys. Rev. B **64**, 012301 (2001).
[28] T. Scopigno *et al.*, Phys. Rev. Lett. **94**, 155301 (2005).
[29] E. G. D. Cohen *et al.*, Phys.Rev. Lett. **59**, 2872 (1987).
[30] T. E. Faber *Introduction to the theory of liquid metals* (Cambridge university press.) 162-165 (1972).